Hydrogen Production from Photo Splitting of Water Using the Ga-incorporated TiO_2s Prepared by a Solvothermal Method and Their Characteristics

Jinho Chae, Juhyun Lee, Jong Hwa Jeong,† and Misook Kang*

Department of Chemistry, College of Science, Yeungnam University, Gyeongsan, Gyeongbuk 712-749, Korea
**E-mail: mskang@ynu.ac.kr*
†Department of Chemistry, Kyungpook National University, Daegu 702-701, Korea
Received November 17, 2008, Accepted December 16, 2008

This study investigated the production of hydrogen over Ga (1.0, 2.0, and 5.0 mol%)-TiO_2 photocatalysts prepared by a solvothermal method. The absorption band was slightly blue-shifted upon the incorporation of the gallium ions, but the intensity of the photoluminescence (PL) curves of Ga-incorporated TiO_2s was distinguishably smaller, with the smallest case being the 2.0 mol% Ga-TiO_2, which was related to the recombination between the excited electrons and holes. H_2 evolution from photo splitting of water over Ga-incorporated TiO_2 in the liquid system was enhanced, compared to that over pure TiO_2; particularly, the production of 5.6 mL of H_2 gas after 8 h when 1.5 g of the 2.0 mol% Ga-incorporated TiO_2 was used.

Key Words: Ga-incorporated TiO_2, Photocatalysis, Water splitting, H_2 production

Introduction

In future, use of energy from hydrogen should increase as it is environmentally friendly. The technology for generating hydrogen by the splitting of water using a photocatalyst has attracted much attention. The principle of photocatalytic water decomposition is based on the conversion of light energy into electricity upon exposure of a semiconductor to light. Light results in the intrinsic ionization of *n*-type semiconducting materials over the band gap, leading to the formation of electrons and electron holes in the conduction and valence bands, respectively.[1] The light-induced electron holes split water molecules into oxygen and hydrogen ions. Simultaneously, the electrons which reduce the hydrogen ions generated to hydrogen gas. To trigger this reaction, the energy of the absorbed photon must be at least 1.23 eV ($E_t = \Delta G^\circ(H_2O)/2N_A$; $\Delta G^\circ(H_2O) = 237.141$ kJ mol^{-1}; N_A = Avogadro's number = 6.022×10^{23} mol^{-1}).[1] The optimized band gap for high hydrogen production is below 2.0 eV. The photocatalytic formation of hydrogen and oxygen on semiconductors, such as $MTiO_3$[2] and $MTaO_2N$,[3-7] (where M = alkaline or transition metals) has been widely investigated due to the low band gap and high corrosion resistance of these semiconductor materials. However, the photocatalytic decomposition of water (H_2O) on a TiO_2 photocatalyst is ineffective as the amount of hydrogen produced is limited by the rapid recombination of holes and electrons, resulting in the formation of water.

To overcome this rapid recombination in water splitting, more investigations into the production of hydrogen *via* methanol or ethanol photodecompositions to upgrade hydrogen production, not water, have focused on modified (Ag or Cu)-doped TiO_2[8-11] which can be used to activate the photocatalysts, using UV light with longer wavelengths and noble metal (Pd, Pt, Rh)-doped TiO_2,[12-14] which have relatively high activity and chemical stability under UV irradiation. The new materials, Ag-TiO_2 and Cu-TiO_2, where Ag_xO and Cu_xO were substituted into a TiO_2 framework, were investigated as conducting components to reduce the large band gap of pure TiO_2. As a result, the Ag and Cu components were found to be very useful for the production of H_2 gas in a methanol photodecomposition system; the productions reached 17,000 μmol and 16,000 μmol after 24 h over Ag/TiO_2 and Cu/TiO_2, respectively. Zou and Ikuma have reported that the activity for hydrogen generation from water/alcohols is greatly improved on Pt/TiO_2, synthesized by a cold plasma method,[12] and the highest rate of H_2 production was also obtained from the Pt-deposited TiO_2 that was formed by the formaldehyde method,[13] respectively. Particularly, Idriss[14] compared the hydrogen production from photo-splitting of ethanol between Pd, Pt, and Rh/TiO_2s. The addition of Pd or Pt dramatically increased the production of hydrogen and a quantum yield of about 10% was reached at 350 K. On the contrary, the Rh doped TiO_2 is far less active, however, this value was still low in the economic evaluation, therefore, attempts were made to upgrade the production of H_2 within a shorter time. In addition, photo splitting of the light hydrocarbons, such as methanol and ethanol, are not environmentally desirable because of the emission of CO and CO_2 during the photoreaction. Additionally, noble metals have high cost. Thus there is an urgent need for the development of new photocatalysts with low cost, that are environmentally friendly, and that possess greater hydrogen-producing activity under visible light irradiation.

We have tried to prepare a new catalyst, the Ga (0, 1, 2, and 5mol%) incorporated TiO_2 photocatalysts with an anatase structure, using a solvothermal method to reduce rapid recombination of holes and electrons and to lower material cost. To determine the relationship between the gallium species and the catalytic performance for the production of H_2, the Ga-TiO_2 photocatalysts were examined using X-ray diffraction analysis (XRD), X-ray photon spectroscopy (XPS), UV-visible spectroscopy, and Photoluminescence (PL) spectroscopy. Hydrogen was generated from photodecomposition of water over Ga-TiO_2 photocatalysts, and the optimum con-

ditions for improvement of hydrogen production were discussed.

Experimental Section

Preparation of TiO_2 and Ga-TiO_2 photocatalysts. Ga-incorporated TiO_2s with various mol fractions of gallium were prepared using a common solvothermal method as shown in Figure 1. To prepare the sol mixture, titanium tetraisopropoxide (TTIP, 99.95%, Junsei Chemical, Tokyo, Japan) and gallium chloride ($GaCl_3$, 99.50%, Junsei Chemical, Tokyo, Japan) were used as the titanium and silicon precursors, respectively, with ethanol as the solvent. 1.0, 2.0, and 5.0 mol% of the gallium chloride, and 0.5 mol TTIP were added to 250 mL distilled water stepwise and then homogeneously stirred for 2 h. Ammonium hydroxide was added and the pH maintained at 9.0 for rapid hydrolysis. The final solution was homogeneously stirred and then moved to an autoclave for thermal treatment. TTTIP and gallium chloride were hydrolyzed *via* the OH group during thermal treatment at 200 °C for 8 h under a nitrogen environment with a pressure of about 10 atm. The resulting precipitate was washed with distilled water until pH = 7.0 and then dried at 100 °C for 24 h.

Characteristics of TiO_2 and Ga-TiO_2 photocatalysts. The synthesized TiO_2 and Ga-incorporated TiO_2 powders were subjected to XRD (model PW 1830; Philips, Amsterdam, The Netherlands), with nickel-filtered Cu$K\alpha$ radiation (30 kV, 30 mA) at 2θ angles from 5 to 70°, with a scan speed of 10° min^{-1} and time constant of 1 s. The sizes and shapes of the TiO_2 and Ga-incorporated TiO_2 particles were determined by using scanning electron microscopy (SEM, model JEOL-JSM35 CF; Tokyo, Japan). High-resolution transmission electron microscopy (TEM) images of the nanometer-sized samples were obtained on a JEOL 2000EX transmission electron microscope operated at 200 kV. The Brunauer, Emmett and Teller (BET) surface areas and pore size distributions (PSDs) of the TiO_2 and Ga-incorporated TiO_2 powders were measured by nitrogen gas adsorption using a continuous flow method; a chromatograph equipped with a thermal conductivity detector (TCD), at liquid-nitrogen temperature, was carried out. A mixture of nitrogen and helium was used as the carrier gas with a MicroMetrics Gemini 2375 (Londonderry, NH, USA). The sample was treated at 350 °C for 3 h prior to nitrogen adsorption. The UV-visible spectra of the TiO_2 and Ga-incorporated TiO_2 powders were obtained using a Shimadzu MPS-2000 spectrometer (Kyoto, Japan) with a reflectance sphere, over the special range 200 to 800 nm. Photoluminescence (PL) spectroscopy measurements of the TiO_2 and Ga-incorporated TiO_2 powders were also conducted to examine the number of photo-excited electron hole pairs for all of the samples. 1.0 mm pellet type samples were measured at room temperature using a He-Cd laser source at a wavelength of 325 nm. X-ray photon spectroscopy (XPS) measurements of Ga2p, Ti2p, and O1s were recorded with a ESCA 2000 (VG MicroTech, Oxford, UK) system, equipped with a non-monochromatic Al$K\alpha$ (1486.6 eV) X-ray source. The TiO_2 and Ga-TiO_2 powders were pelletized, at 1.2×10^{4} kPa for 1 min, and the 1.0-mm pellets were then maintained overnight in a vacuum (1.0×10^{-7} Pa) to remove water molecules from the surface prior to measurement. The base pressure of the ESCA system was below 1×10^{-9} Pa. Experiments were recorded with a 200-W source power and an angular acceptance of ±5°. The analyzer axis made an angle of 90° with the specimen surface. Wide scan spectra were measured over a binding energy range of 0 to 1200 eV, with pass energy of 100.0 eV. The Ar^+ bombardment of the TiO_2 and Ga-TiO_2 was performed with an ion current of 70 to 100 nA, over an area of 10.0 × 10.0 mm, with a total sputter time of 2400 s divided into 60 intervals. A Shirley function was used to subtract the

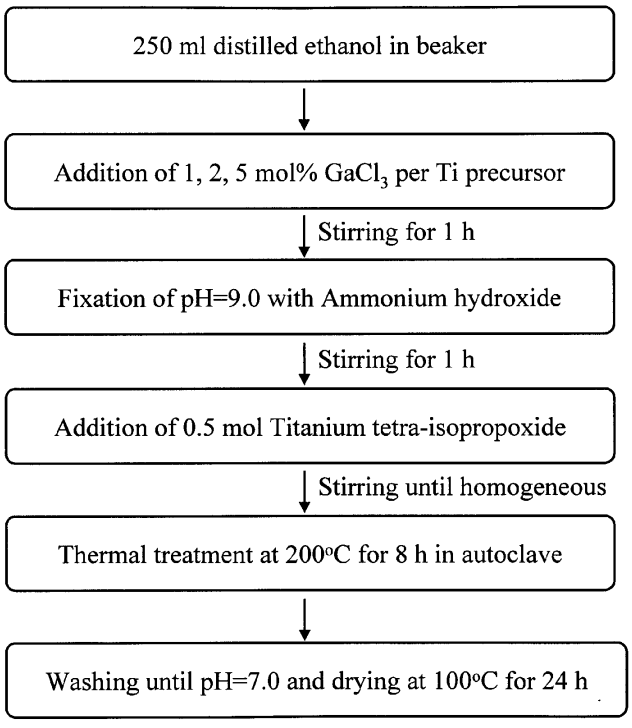

Figure 1. The preparation of Ga-TiO_2 using a conventional solvothermal method.

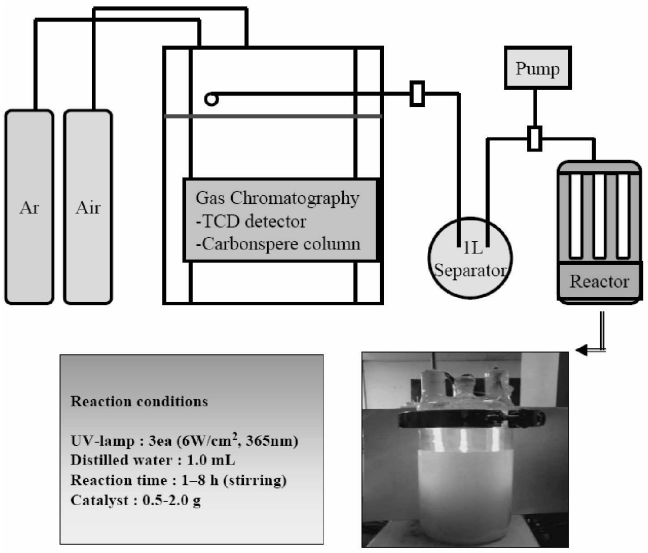

Figure 2. The liquid photoreactor used for H_2 production *via* photo splitting of water.

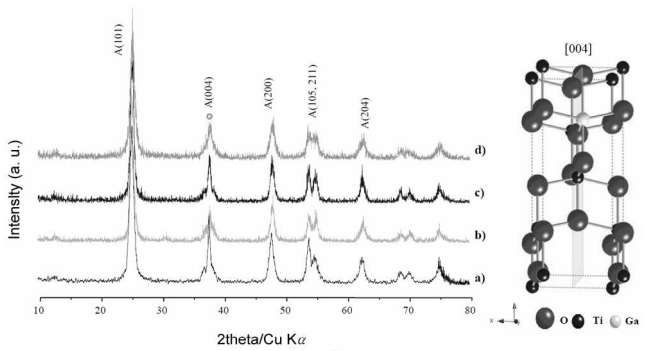

Figure 3. XRD patterns of pure TiO_2 and Ga-TiO_2 as-synthesized: (a) TiO_2, (b) 1.0 mol% Ga-TiO_2, (c) 2.0 mol% Ga-TiO_2, and (d) 5.0 mol% Ga-TiO_2.

background in the XPS data analysis. The O1s, Ti2p, and Ga2p XPS signals were fitted using mixed Lorentzian-Gaussian curves.

H_2 production from photo splitting of water over TiO_2 and Ga-TiO_2. The photo splitting of water was performed using a liquid photo reactor designed in our laboratory as shown in Figure 2. For photo splitting of water, 0.5~2.0 g of the powdered TiO_2 and Ga-TiO_2 photocatalysts were added to 1.0 L of distilled water in a 2.0-L Pyrex reactor. UV-lamps (6 x 3 W cm^{-2} = 18 W cm^{-2}, 30 cm length × 2.0 cm diameter; Shinan, Sunchun, Korea) with emitting radiation at 365 nm were used. The photo splitting of water was conducted for 1~7 h, with stirring, with hydrogen evolution determined after 1 h. The hydrogen gas (H_2) produced during water photo splitting was analyzed using a TCD-type gas chromatograph (GC, model DS 6200; Donam Instruments Inc., Gyeonngi-do, Korea). To determine the products and intermediates, the GC was directly connected to the water decomposition reactor. The following GC conditions were used: TCD detector; Carbosphere column (Alltech, Deerfield, IL, USA); 140 °C injection temp; 120 °C initial temp.; 120 °C final temp.; 150 °C detector temp.

Table 1. The atomic composition of the TiO_2 and Ga-TiO_2 photocatalysts.

Catalyst Characteristics		TiO_2 Anatase	1.0mol% Ga-TiO_2	2.0mol% Ga-TiO_2	5.0mol% Ga-TiO_2
Composition on surface (atomic %)	Ti	27.21	26.98	25.26	26.04
	O	69.23	68.25	69.76	68.35
	Ca	-	0.11	0.24	0.61
Surface Area (m^2/g)		65.56	70.19	83.81	107.07
Pore Volume (mL/g)		0.0235	0.0343	0.0411	0.0522

Results and Discussion

Characteristics of TiO_2 and Ga-TiO_2 photocatalysts. Figure 3 shows the crystallinity obtained from the XRD patterns of TiO_2 and the 1.0, 2.0, and 5.0 mol% Ga-incorporated TiO_2 powders. The Ga-incorporated TiO_2 particles exhibited a pure structure of anatase without being thermally treated above 500 °C. The anatase structure had peaks at 25.3, 38.0, 48.2, 54, 63, and 68°, which are assigned to the (d_{101}), (d_{004}), (d_{200}), (d_{105}), (d_{211}), and (d_{204}) planes, respectively. In spite of the addition of the gallium components to the TiO_2 framework, no peaks assigned to Ga_2O_3 (mainly peaks: 2theta = 45 and 52°), which would indicate its presence on the external surface of the anatase framework, were shown, indicating that the gallium ions were safely incorporated into the titanium anatase framework. However, the [004] plane peak intensities were smaller with the amount of gallium components compared to other peaks, indicating that the smaller gallium ions insert to [004] site by substitution of the larger titanium ions, as shown in framework figure beside. Compared with the line width of peaks for the anatase structure of pure TiO_2, those of the Ga-TiO_2s decreased, resulting from the difference between

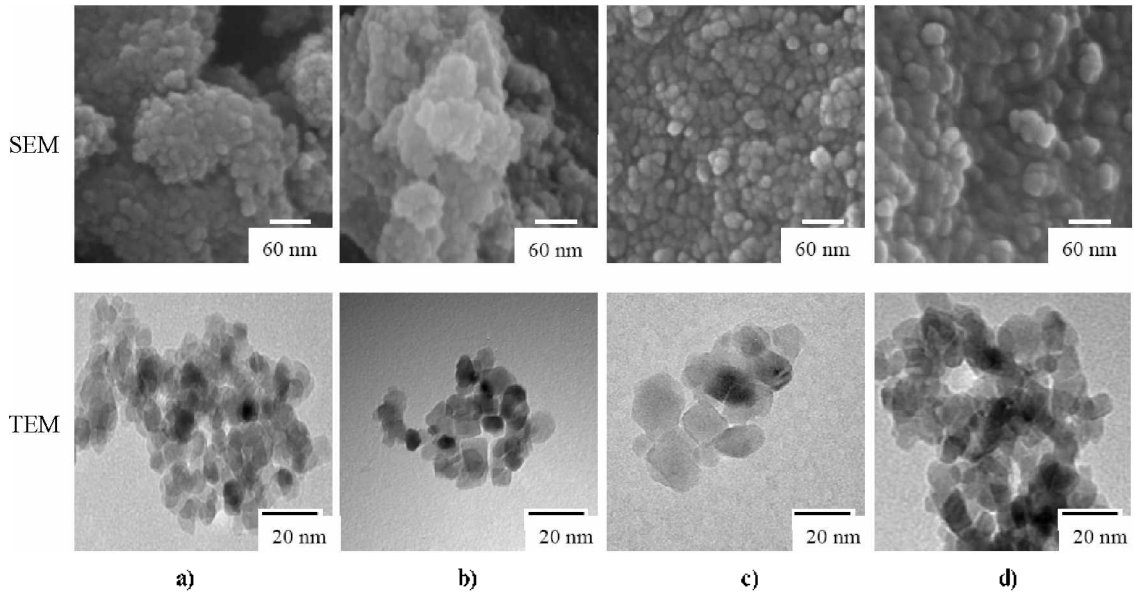

Figure 4. SEM and TEM images of TiO_2 and Ga-TiO_2 as-synthesized: (a) pure TiO_2, (b) 1.0 mol% Ga-TiO_2, (c) 2.0 mol% Ga-TiO_2, and (d) 5.0 mol% Ga-TiO_2.

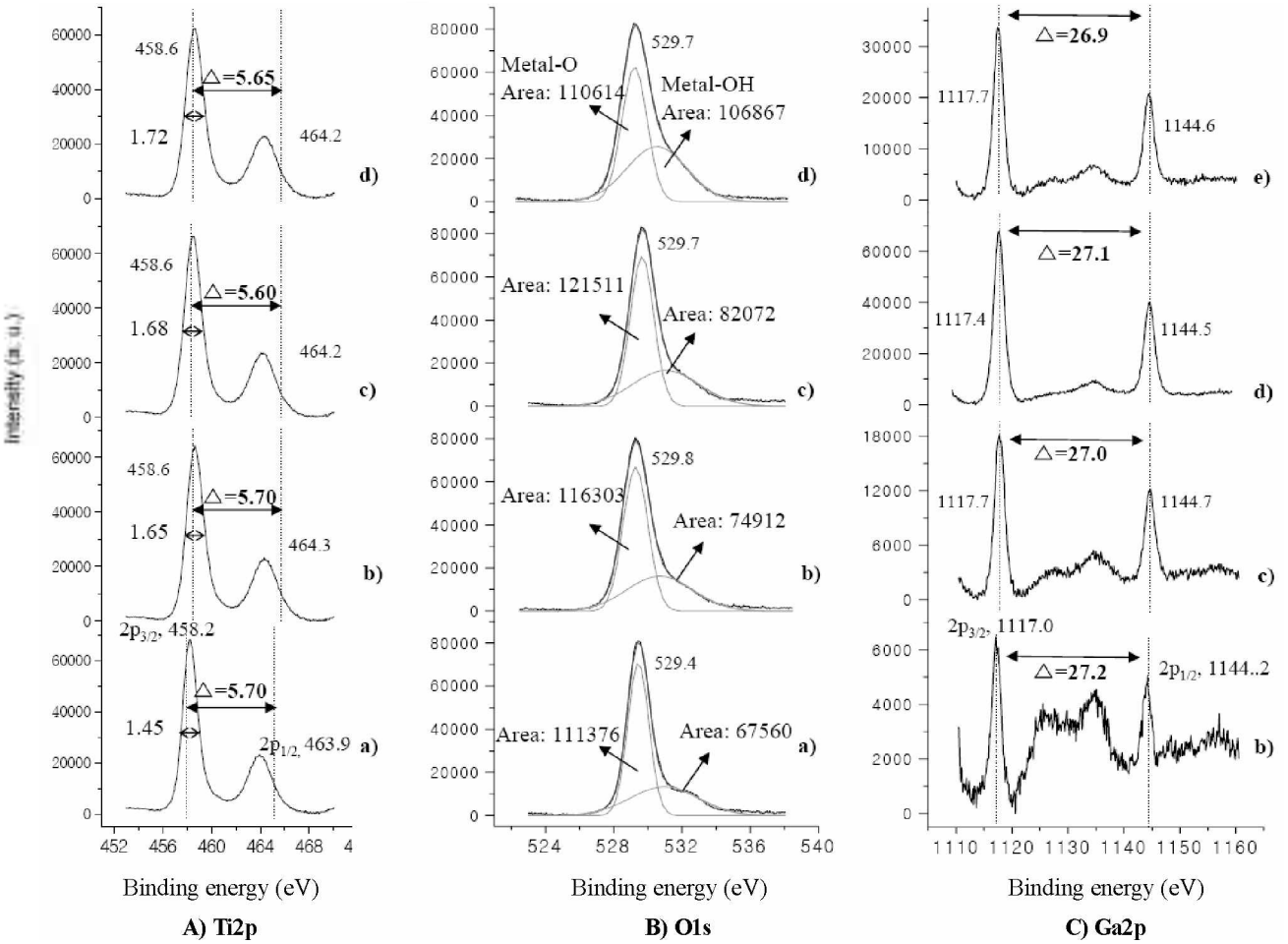

Figure 5. XPS of TiO_2 and Ga-TiO_2 as-synthesized: (A) For Ti2p, (B) For O1s, and (C) For Ga2p; (a) pure TiO_2, (b) 1.0 mol% Ga-TiO_2, (c) 2.0 mol% Ga-TiO_2, and (d) 5.0 mol% Ga-TiO_2.

the ionic radii of Ti^{4+} (68 pm) and Ga^{3+} (62 pm). Generally, the larger the line-broadening of the peaks, the smaller the crystalline domain sizes. The line broadening of the peak of the (101) index is related to the size of the hexagonal crystalline phase. The full width at half maximum (FWHM) height of the peak at 2 theta = 25.3° was observed to be 1.593 degrees. Scherrer's equation, $t = 0.9\lambda/\beta\cos\theta$, where $\lambda$is the wavelength of the incident X-rays, $\beta$is the full width at half maximum height in radians, and the θ is the diffraction angle, was used to determine the crystalline domain size. The calculated crystalline domain sizes were 17, 25, 24, and 23 nm for TiO_2 and the 1.0, 2.0, and 5.0 mol% Ga-incorporated TiO_2, respectively.

Figure 4 shows the SEM and TEM photographs of the particle shapes of TiO_2 and the 1.0, 2.0, and 5.0 mol% Ga-incorporated TiO_2. A relatively uniform mixture of rhombic and cubic particles whose sizes were distributed within the range of 10-15 nm was shown in these photographs. When the gallium components were added, the particles coagulated to assume a cubic type shape and their size increased slightly, in the order of pure TiO_2 < 1.0 mol% Ga-TiO_2 > 5.0 mol% Ga-TiO_2 > 2.0 mol% Ga-TiO_2. This corresponds to the results of the XRD analysis shown in Figure 3.

Table 1 summarizes the physical properties of the TiO_2 and 1.0, 2.0, and 5.0 mol% Ga-incorporated TiO_2 powders. From the energy dispersive analysis of X-rays (EDAX), the true atomic ratios of gallium/titanium in the 1.0, 2.0, and 5.0 mol% Ga-incorporated TiO_2 powders were found to be 0.41, 0.95, and 2.34 mol%, respectively, indicating that insertion of the gallium ion into TiO_2 framework is not facile. The volume increased with the addition of gallium as did the BET surface areas. Generally, surface area is strongly related to the particle size; when the particle size decreases, the surface area increases, however, was not the case in our results.

Quantitative XPS analyses of the TiO_2 and Ga-TiO_2 particles were performed, with the typical survey and high-resolution spectra shown in Figure 5. The $Ti2p_{1/2}$ and $Ti2p_{3/2}$ spin-orbital splitting photoelectrons for anatase TiO_2s were located at binding energies of 463.9 and 458.2 eV, respectively, and assigned to the presence of typical Ti^{4+}. In Ga-TiO_2, the bands were broad when the gallium ion was added, and shifted slightly to a higher binding energy of 458.6 and 464.3 eV for $Ti2p_{3/2}$ and $Ti2p_{1/2}$, respectively, which was assigned to Ti^{3-}. The differences (delta) in binding energies between $Ti2p_{3/2}$ and $Ti2p_{1/2}$ were distributed in the range of 5.60 ~ 5.70 in all catalysts. The measured FWHM of the $Ti2p_{3/2}$ peak was remarkably larger in the Ga-TiO_2 than in pure TiO_2. In general, a greater FWHM implies a greater amount of less-oxidized metals.[15] The FWHM increased in the order of pure TiO_2(1.45) < 1.0 mol% Ga-TiO_2(1.65) < 2.0

mol% Ga-TiO_2(1.68) < 5.0 mol% Ga-TiO_2(1.72). This indicated that the oxidation state of the Ti ion was lessened when the gallium ion was added, strongly effecting photocatalysis. The bond distance between Ti^{3+} and O maybe more loose than the bond between Ti^{4+} and O, and so the electron transfer from oxygen to titanium occurs readily, and consequently the photocatalysis could be improved. The O1s region was separated into two contributions: metal (Ti^{4-} or Ti^{3+})-O (529.4eV) in the metal oxide and metal-OH (532.0 eV). The ratios of metal-OH/metal-O in the O1s peaks were distinguishably increased in Ga-TiO_2 compared to that in pure TiO_2, increasing in the order of pure TiO_2(0.61) < 1.0 mol% Ga-TiO_2(0.64) < 2.0 mol% Ga-TiO_2(0.68) < 5.0 mol% Ga-TiO_2(0.97). In general, a higher metal-OH peak indicates that the particles are more hydrophilic, and thus produces much more OH radicals during photocatalysis, consequently, its photocatalytic activity can be improved. The sample should be more hydrophilic when the gallium ion is added. In addition, the measured FWHM of the O1s peak was larger in Ga-TiO_2 than in pure TiO_2, similar to that shown for the FWHM of the Ti2p peaks. The $Ga2p_{3/2}$ and $Ga2p_{1/2}$ spin-orbital splitting photoelectrons for anatase Ga-TiO_2 were located at binding energies of 1117 and 1144 eV, respectively, and these bands were assigned to Ga_2O_3.[16] The differences (delta) in binding energies between $Ga2p_{3/2}$ and $Ga2p_{1/2}$ were about 27.0 for all catalysts. The measured FWHM of the $Ga2p_{3/2}$ peak in the Ga-TiO_2 was a little bit larger than that in pure TiO_2.

H_2 production from photo splitting of water over TiO_2 and Ga-TiO_2. The evolution of H_2 from photo splitting of water over the TiO_2 and Ga-TiO_2 photocatalysts with a catalyst's concentration in a batch-type liquid photo system was summarized in Table 2. In Figure 6, no H_2 was collected after photo-decomposition of water for 7 h over pure anatase TiO_2 and 1.0 mol% Ga-TiO_2, while a marked amount of H_2 gas was collected over other Ga-TiO_2s; the amount of H_2 produced reached 3.0 mL over 2.0 mol% Ga-TiO_2, but decreased significantly above 5.0 mol% Ga-TiO_2. The optimized gallium concentration in this study was 2.0 mol% *vs* the titanium molar concentration. The reasons attributed being that 2.0 mol% Ga-TiO_2 have much more hydrophilic property, less oxidized titanium, and smaller recombination between excited electrons and holes. Oxygen evolution corresponded to half the hydrogen, as shown in Figure 6B, confirming the reliability of the experiment. The evolution of H_2 from water photo splitting over the 2.0 mol% Ga-TiO_2 upon the amount of catalyst used was summarized in Table 2. Evolution of H_2 increased as the amount of catalyst used increased, until 1.5 g/L, but decreased above 2.0 g/L. When 0.5 g/L was used, evolved H_2 gas for 1 h was about 0.03~0.05 mL that almost completely stopped after 5 h. H_2 gas was noticeably produced when 1.5 g/L of the catalyst was used, generating 5.6 mL after 8 h, however the produced amount of H_2 gas decreased to 2.1 mL when the amount of catalyst was 2.0 g/L, resulting from a disruption by light scattering. Consequently, the optimized amount of catalyst was 1.5 g/L.

Table 2. Collected H_2 (mL) gases from photo splitting of water over 2.0 mol% Ga-TiO_2 upon the amount of catalyst used.

Reaction time (h)	Amount of catalyst (g/L)		
	0.5 g/L	1.5 g/L	2.0 g/L
After 1 h	0.035	0.936	0.505
2h	0.087	2.081	0.891
3h	0.119	3.017	1.191
4h	0.147	3.718	1.422
5h	0.180	4.297	1.620
6h	0.180	4.770	1.803
7h	0.180	5.195	1.985
8h	0.180	5.609	2.138

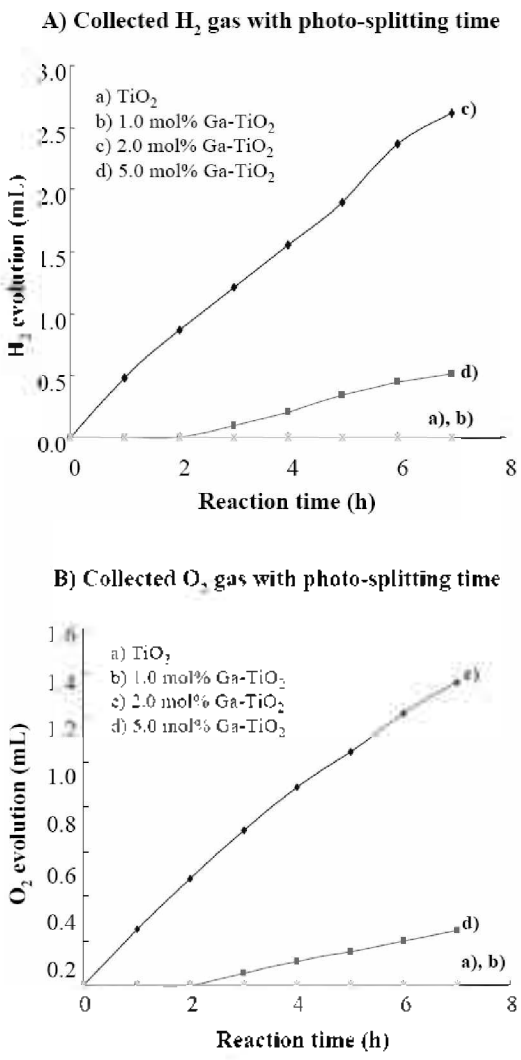

Figure 6. The H_2 evolution from water photo splitting over pure TiO_2 and Ga-TiO_2: (a) pure TiO_2, (b) 1.0 mol% Ga-TiO_2, (c) 2.0 mol% Ga-TiO_2, and (d) 5.0 mol% Ga-TiO_2.

To know the relationship between the hydrogen evolution and spectroscopic property, the UV-visible spectra and the photoluminescence (PL) spectra of the TiO_2 and 1.0, 2.0, and 5.0 mol% Ga-incorporated TiO_2 powders were measured, as shown in Figure 7. In Figure 7A, the absorption band for the tetrahedral symmetry of Ti^{4-} normally appears at around 360 nm. In the spectra of the Ga-incorporated TiO_2, the absorption bands were slightly blue-shifted compared with that of pure TiO_2. Generally, the band gaps in a semiconductor material are closely related to the wavelength range absorbed where the higher the absorption wavelength, the shorter the band

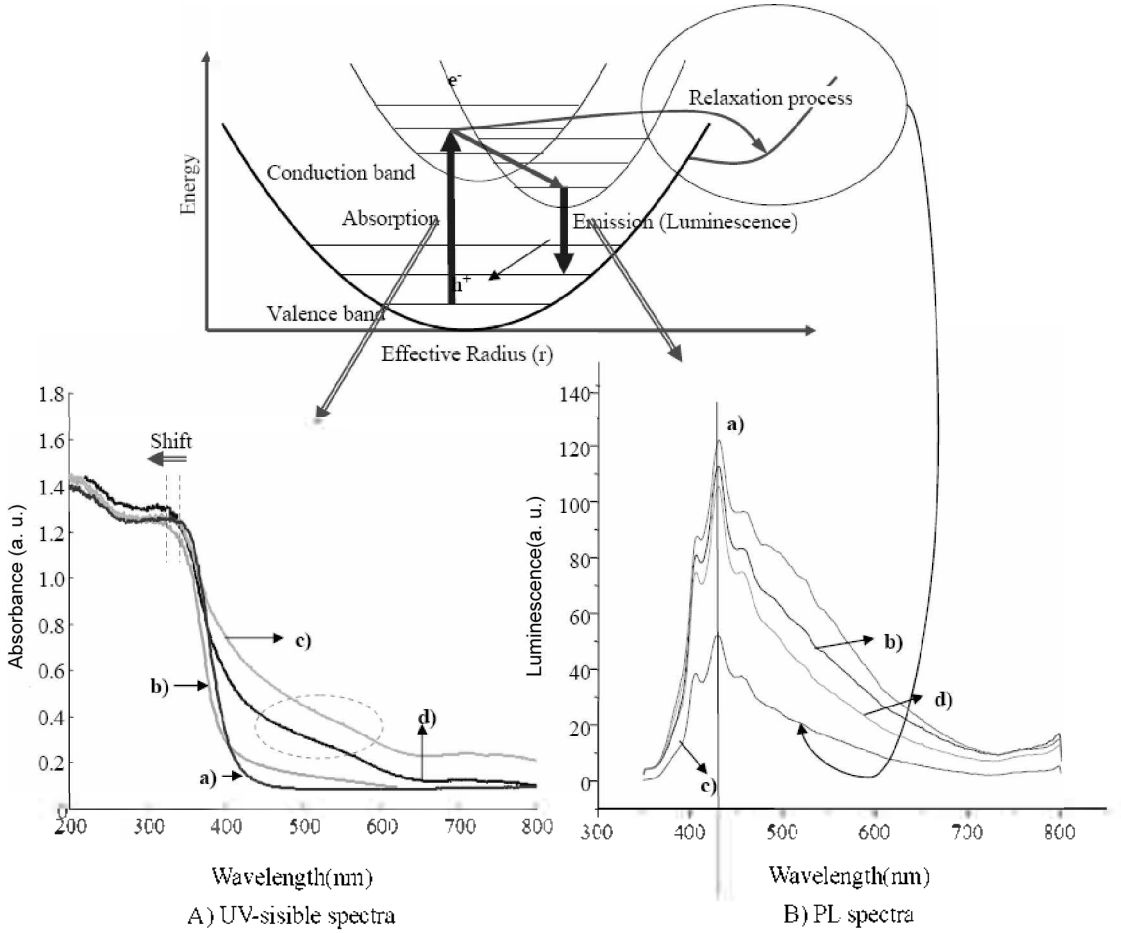

Figure 7. UV-visible (A) and PL (B) spectra of pure TiO_2 and Ga-TiO_2 as-synthesized: (a) pure TiO_2, (b) 1.0 mol% Ga-TiO_2, (c) 2.0 mol% Ga-TiO_2, and (d) 5.0 mol% Ga-TiO_2.

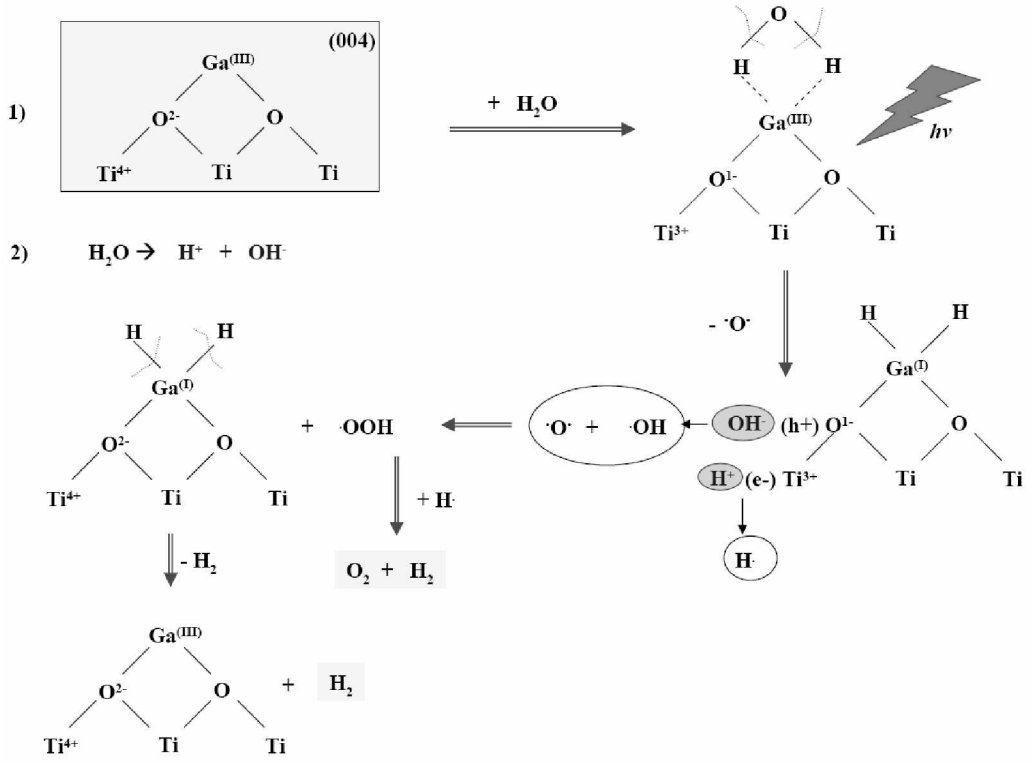

Scheme 1. Expected model for hydrogen production from photo splitting of water.

gap. However, herein it is postulated that the addition of the gallium component did change the band gap energy of the TiO_2 semiconductor rather significantly. Figure 7B presents the photoluminescence (PL) spectra of pure TiO_2 and the Ga-incorporated TiO_2s. The PL curve indicates that the electrons in the valence band transferred to the conduction band, and then the excited electrons were stabilized by photoemission. In general, if the number of the emitted electrons resulting from the recombination between excited electrons and holes is increased, the PL intensity increases, and consequently, the photoactivity decreases.[17] Therefore, there is a strong relationship between PL intensity and photoactivity. In particular, when metal that can capture excited electrons or exhibit conductivity, can called to relaxation process, is present, the PL intensity decreases to a greater extent. In Figure 7B, the PL curve of Ga-TiO_2 was similar to that of pure anatase titania with an emission at 450 nm. The PL intensity of 2.0 mol% Ga-TiO_2 was the smallest and sharpest, most likely due to the gallium atoms playing the role of electron capturers, thereby depressing the recombination process. Consequently, higher photocatalytic activities are to be expected. In the case of pure TiO_2, broad emissions were shown; the band was attributed to the overlapped emission from the higher and lower excited states to the ground states. Consequently, the PL intensity varied depending on whether the added metal acted as an electron capturer or not.

Based on the characteristics, a model is suggested in Scheme 1 to explain the effect of the gallium component existing in the [004] plane of anatase structure for high H_2 production from the photo splitting of water. Generally it is well-known that aluminum or gallium components strongly react with water molecules. If Ga(III) exists in the framework, it easily attracts water molecules. The water molecules are broken by UV-radiation, simultaneously reducing Ga(III) to Ga(I), and transferred to oxygen per radicals. Otherwise the electrons and holes, which generated on the valence and conduction bands on TiO_2, produce OH and H radicals respectively. The OH radicals are transferred to OOH radicals by reaction with oxygen per radicals, and then the hydrogen and oxygen gases evolve by reaction of OOH radicals and H radicals. Finally, Ga(I) is recovered to Ga(III) by decomposition of hydrogen gas.

Conclusions

TiO_2 photocatalysts incorporated with gallium ions were prepared for the production of H_2 gas from photodecomposition of water in a batch-type liquid photo system. The following conclusions can be drawn from this study: the hydrogen production from photo splitting of water was enhanced over the 2.0 mol% Ga-incorporated TiO_2 compared with that over pure TiO_2: 5.6 mL of H_2 gas was collected after 8 h over the 2.0 mol% Ga-incorporated TiO_2 when 1.5 g/L of catalyst was used. From these results, we suggest that hydrogen production from water splitting can be more readily achieved over the Ga-incorporated TiO_2 than over pure TiO_2. Consequently, we found herein that the lower band gap did not always affect the photocatalytic activity and that depressing the recombination between electrons and holes, the hydrophilic properties, and the less-oxidized titanium were more important.

Acknowledgments. This research was supported by the Yeungnam University research grants in No. 208A356007, for which the authors are very grateful.

References

1. Bak, T.; Nowotny, J.; Rekas, M.; Sorrell, C. C. *Int. J. Hydrogen Energy* **2002**, *27*, 991.
2. Mizoguchi, H.; Ueda, K.; Orita, M.; Moon, S. C.; Kajihara, K.; Hirano, M.; Hosono, H. *Mater. Res. Bull.* **2000**, *37*, 2401.
3. Ye, J.; Zou, Z.; Matsushita, A. *Int. J. Hydrogen Energy* **2003**, *28*, 651.
4. Hara, M.; Takata, T.; Kondo, J. N.; Domen, K. *Catal. Today* **2004**, *90*, 313.
5. Hara, M.; Hitoki, G.; Takata, T.; Kondo, J. N.; Kobayashi, H.; Domen, K. *Catal. Today* **2003**, *78*, 555.
6. Yamasita, D.; Takata, T.; Hara, M.; Kondo, J. N.; Domen, K. *Solid State Ionics* **2004**, *172*, 591.
7. Jang, J. S.; Kim, H. G.; Reddy, V. R.; Bae, S. W.; Ji, S. M.; Lee, J. S. *J. Catal.* **2005**, *231*, 213.
8. Park, M.-S.; Kang, M. *Int. J. Hydrogen Energy* **2007**, *32*, 4840.
9. Choi, H.-J.; Kang, M. *Int. J. Hydrogen Energy* **2007**, *32*, 3841.
10. Jeon, M.-K.; Park, J.-W.; Kang, M. *J. Ind. Eng. Chem.* **2007**, *13*, 84.
11. Park, J.-W.; Kang, M. *Mater. Lett.* **2008**, *62*, 183.
12. Zou, J.-J.; He, H.; Cui, L.; Du, H.-Y. *Int. J. Hydrogen Energy* **2007**, *32*, 1762.
13. Ikuma, Y.; Bessho, H. *Int. J. Hydrogen Energy* **2007**, *32*, 2689.
14. Yang, Y. Z.; Chang, C.-H.; Idriss, H. *Appl. Catal. B: Environ.* **2006**, *67*, 217.
15. Wu, N.-L.; Lee, M.-S.; Pon, Z.-J.; Hsu, J.-Z. *J. Photochem. Photobiol. A: Chem.* **2004**, *163*, 277.
16. Mouider, J. F.; Stickle, W. F.; Soboi, P. E.; Bomben, K. D. *Handbook of X-ray Photoelectron Spectroscopy*; Perkin-Elmer Coporation: USA, 1992; p 90.
17. Lee, B.-Y.; Park, S.-H.; Lee, S.-C.; Kang, M.; Park, C.-H.; Choung, S.-J. *J. Ind. Eng. Chem.* **2003**, *20*, 812.